SPECIAL BRIEF NOTE

ON THE NEAR-WAKE TOPOLOGY OF AN OSCILLATING CYLINDER

J. Sheridan and J. Carberry

Monash University, Melbourne, Australia

and

J.-C. Lin and D. Rockwell

Lehigh University, Bethlehem, PA, U.S.A.

Instantaneous patterns of vorticity and topology of streamlines, obtained via a technique of high-image-density particle image velocimetry, are employed to characterize quantitatively the near-wake of a cylinder undergoing large amplitude oscillations in a uniform flow.

1. INTRODUCTION

During the past few decades, substantial advances have been made in our understanding of the near-wake structure of an oscillating cylinder. The concept of locked-on vortex formation has been reviewed by Sarpkaya (1979), Bearman (1984), Rockwell (1990), Griffin & Hall (1991, 1995) and Hall & Griffin (1993). Emphasis has been on qualitative visualization of the near-wake, with the intent of gaining an understanding of the loading of the cylinder. Zdravkovich (1982), Öngoeren & Rockwell (1988) and Williamson & Roshko (1988) interpret abrupt changes in the process of vortex formation in the context of rapid changes in the phase and magnitude of the fluctuating lift observed in previous measurements.

Little attention has been devoted to quantitative assessment of the near-wake structure in terms of instantaneous vorticity distributions and streamline patterns interpreted within a framework based on topological concepts. Rockwell (1993) provides examples of this approach for PIV imaging of quasi-two-dimensional and three-dimensional near-wakes, and Gu *et al.* (1994) describe a possible mechanism for a switch in timing of quasi-two-dimensional vortex formation from an oscillating cylinder based on instantaneous patterns of vorticity and streamline patterns exhibiting well-defined saddle points and foci. These studies, at Reynolds numbers Re = 185 and 5000, focused on low amplitudes of oscillation $A/D = 0.2$, for which consistent lock-on of the vortex formation process was attainable. In essence, an increase in excitation frequency of the cylinder results in formation of the initial concentration of vorticity at a location closer to the base of the cylinder until a limiting position is attained; then, the initially formed concentration suddenly switches to the

opposite side of the cylinder. Lu & Dalton (1996) have numerically simulated the near-wake structure at Re = 185, 500 and 1000. For a range of frequency ratio f_e/f_0, and at a somewhat larger amplitude $A/D = 0.4$, their patterns of vorticity concentrations confirm this mechanism of vortex switching. Blackburn & Henderson (1995) show a generally similar process of switching of the vorticity contours at Re = 500 and amplitude $A/D = 0.5$, and emphasize the importance of generation of vorticity from the base of the cylinder. It should be noted that these quantitative assessments of the near-wake patterns are in general accord with interpretations based on qualitative flow visualization, for the most part at low values of amplitude A/D. They include the original hypothesis of the switching mechanism by Zdravkovich (1982), its possible occurrence for cylinders of various cross-sections by Öngoeren & Rockwell (1988), and existence of a very similar mechanism for the near-wake vortices formed from a blunt trailing-edge subjected to controlled oscillations by Staubli & Rockwell (1989).

The present investigation represents an extension of the approach of Gu *et al.* & Rockwell (1994) to larger values of excitation amplitude, with the intent of characterizing the near-wake vorticity distribution and streamline topology during the oscillation cycle of the cylinder.

2. EXPERIMENTAL SYSTEM AND TECHNIQUES

The test-section of the Lehigh University water channel, which housed the oscillating cylinder, had a width of 210 mm and a water depth of 527 mm. The nominal position of the horizontal cylinder was at the mid-depth beneath the free surface. It was mounted on a vertical excitation arm, which was connected to a traverse table, driven by a computer-controlled motor. In order to ensure that this forcing system did not interfere with the flow pattern, it was located outside a false wall. Design of the junction between the cylinder and the vertical arm precluded leakage from the test-section to the surrounding fluid. This test-section housing the cylinder was, in turn, mounted within a large-scale water channel having an inlet width of 1828 mm and a depth of 584 mm. In order to optimize the flow quality, it passed through two successive 3:1 contractions before entering the test-section that housed the cylinder.

The cylinder diameter was $D = 12.7$ mm, and the free-stream velocity $U = 40.7$ mm/s, giving a value of Reynolds number Re = 517. Acquisition of quantitative images involved application of a scanning laser version of the PIV technique, described by Rockwell *et al.* (1993). The beam from a continuous wavelength argon-ion laser (25 W) impinged upon a rotating mirror having 48 facets, which yielded a high-speed scanning of the beam at a frequency of 7.63 cycles/s.

Particle images were generated by seeding the flow with 12 μm diameter metallic-coated hollow spheres. Images were acquired using a 35 mm Nikon F-4 camera at a shutter speed of 1/60 s and at $f^\# = 5.6$. To overcome difficulties associated with negative regions of velocity, a rotating bias mirror was located in front of the camera lens, which had a magnification of $M = 1:9.5$. High-resolution film at 300 lines/mm was employed. The particle images on the film had a density greater than 60 images/mm^2. During interrogation of the images to obtain the instantaneous velocity vectors, a single-frame cross-correlation technique was employed, with 50% overlap of the interrogation windows. The window was maintained at dimensions 0.85 mm × 0.85 mm, and the corresponding window size in the plane of the laser sheet was 1.66 mm × 1.66 mm. This process yielded approximately 3 100 velocity vectors in each image. The effective grid size was $\Delta = 0.85$ mm. As shown by Lin

& Rockwell (1997), the dimensionless grid Δ/D must be sufficiently small in order to properly resolve meaningful scales of vortices present in the near-wake and to evaluate the dimensionless circulation of the vortices.

3. PATTERNS OF INSTANTANEOUS VORTICITY IN THE NEAR-WAKE

Figure 1 shows one-half cycle of the cylinder oscillation at a dimensionless amplitude $A/D = 1$ and a frequency ratio $f_e/f_0 = 1$, in which f_e is the excitation frequency and f_0 is the inherent vortex formation frequency from the stationary cylinder. The time sequence of images extends from the maximum-positive to maximum-negative position of the cylinder. Correspondingly, the angle of the incident flow relative to the cylinder changes and the wake responds to a global, swinging motion.

In the first image, a train of negative (dashed line) vorticity concentrations, each having a rotation in the clockwise direction, extends from the top to the bottom of the image. They have been shed during a previous portion of the oscillation. These small-scale vorticity concentrations tend to agglomerate into two moderate-scale clusters designated as A and B. The evolution of these clusters is indicated in the second and third images, below the first. In the meantime, vorticity concentration C forms at the base of the cylinder, as shown in the first image. As the cylinder moves downward, the onset of separation of the vorticity layer that feeds into the vorticity cluster C moves to a location approximately coincident with the base of the cylinder, i.e., at $\theta = 180°$. The third image shows that concentration C is distorted somewhat as it starts to form a counter-rotating vortex pair with vorticity cluster B and, in the fourth image, the formation of the vortex pair B–C is complete. It is interesting to note that, at the instant corresponding to the third image, the cylinder has reached the mid-point of its downward stroke, at which time the forward stagnation point presumably has reached its maximum angular displacement. Thus, the global rotation of the entire wake changes direction and begins to move back towards the horizontal. Vorticity cluster C is shed soon after this mid-point of the stroke is attained. Moreover, a subsequent concentration of vorticity E is formed from the upper-shoulder of the cylinder in images 2–5, and it takes on a relatively mature form in the fifth image. The pattern of vortices D–E shown in the fifth image generally is a mirror image of the pattern formed by B–C in the first image.

Central to the formation of the counter-rotating vortex pair is the formation of two clusters of vorticity, e.g., A and B or C and D, during each half-cycle of the cylinder oscillation. These are most likely attributable to the fact that the acceleration has its maximum magnitudes at the extreme positions of the cylinder and a value of zero at the half-point of the cylinder trajectory during its oscillation cycle. An open issue is the degree to which the Kelvin–Helmholtz instability of the highly accelerated vorticity layer separating from the cylinder contributes to the formation of these two clusters of vorticity during each half-cycle. The presence of two small-scale concentrations of vorticity in the vorticity cluster B in the first image suggests that the wavelength of the small-scale concentrations due to the K–H instability is smaller than that between the two moderate-scale clusters of vorticity that eventually evolve. Nevertheless, the possibility exists for agglomeration of the smallest-scale K–H vortices into the larger-scale clusters through a mechanism of vortex pairing, well-known to occur in an unstable, separated vorticity layer (Brown & Roshko 1974).

Corresponding streamline patterns and a representative velocity field are shown in Figure 2. Images in the left column correspond to the laboratory frame. Neither the streamline pattern nor the velocity field clearly indicate the existence of a well-defined
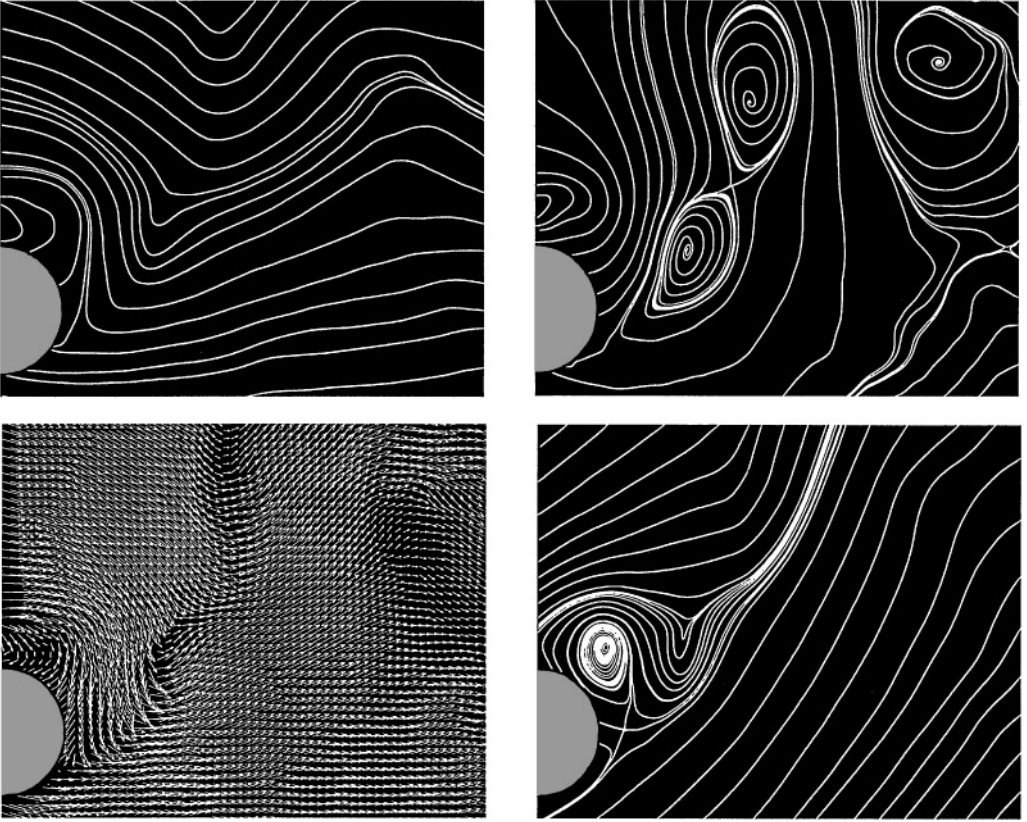
Figure 2. Streamline patterns and representative velocity field corresponding to third image of Figure 1. Images in left column correspond to laboratory frame of observation. Top image in right column is in a frame moving with incident freestream velocity, and bottom image in right column corresponds to a frame moving with instantaneous vertical velocity of cylinder.

vorticity concentration. On the other hand, the image at the upper-right, in a reference frame moving with the incident free-stream velocity U, indicates existence of the major concentrations of vorticity B, C and D in the near-wake. Clearly defined saddle points exist beneath vortex B and between vortices C and D. Furthermore, an alleyway flow, designated by upward-oriented streamlines, exists between vortices B and C of opposite sense, compatible with the velocity induced by the counter-rotating pair B–C. Comparing the foci (centres) of this system of vortices with the corresponding centroids of the vorticity concentrations B, C and D in Figure 1 shows that they are approximately coincident. The streamline pattern at the upper-right of Figure 2 suggests the existence of vortex E, corresponding to the vorticity contours in Figure 1. The apparent focus of the streamline pattern is, however, substantially shifted to the left relative to the centroid of the vorticity concentration. The image at the lower right of Figure 2, corresponding to a reference frame moving with the instantaneous vertical velocity of the cylinder, does have a focus approximately coincident with the centroid of vorticity concentration E, and a well-defined saddle point occurs beneath the focus of the streamline pattern of Figure 2. On the other hand, the existence of all remaining vorticity concentrations B, C and D is not properly represented in this reference frame. We therefore conclude that no single reference frame can adequately

represent the entire vortex system in the near-wake and in the immediate vicinity of the cylinder surface. Moreover, this observation emphasizes that the streamline topology and associated critical points are most meaningful when interpreted in conjunction with contours of constant vorticity.

The principal features of formation of the counter-rotating vortex pair were first identified for cross-flow oscillations of a cylinder by Williamson & Roshko (1988). The schematics of their 2P mode (see their figures 11 and 12), based on particle streak visualization in the different reference frames of the cylinder (see their figures 8, 13 and 14), are in general agreement with the patterns of Figure 1. Moreover, we note that the dimensionless amplitude and frequency parameters, for which their 2P mode occurs, i.e., at $f_e/f_0 = 1\cdot0$ and $A/D = 1\cdot0$ are consistent with their regime map. Such formation of counter-rotating vortex pairs appears to be an inherent feature of wakes from cylinders oscillating at large amplitude. Indeed, very similar pairs are generated for in-line oscillations of a cylinder, as found by Griffin & Ramberg (1974) and Öngoeren & Rockwell (1988), in soap film flow by Couder & Basdevant (1986) and for in-line oscillations generated by a sound wave past a cylinder by De Temple-Laake & Eckelmann (1989).

These features of vortex formation in the near-wake seem to be distinct from those occurring at relatively low amplitudes, addressed experimentally by Gu *et al.* (1994) and numerically by Lu & Dalton (1996) and Blackburn & Henderson (1995). The concept postulated by Gu *et al.* (1994), addressed in the Introduction in the context of previous studies, is that the initially formed vortex moves closer to the cylinder with increasing excitation frequency, until a limiting condition is reached and a switch in timing of the initial vortex from one side of the cylinder to the other occurs. Patterns of instantaneous vorticity of Gu *et al.* (1994), Lu & Dalton (1996) and Blackburn & Henderson (1995) do not exhibit formation of counter-rotating vortex pairs. In general, the vorticity layers separate from the shoulders of the cylinder, in contrast to the case of large amplitude shown herein, where the separation point appears to move to the base of the cylinder at sufficiently high amplitude. Moreover, the separated vorticity layers maintain their integrity at these low amplitudes, though, as indicated by Gu *et al.* (1994), they may exhibit Kelvin–Helmholtz instabilities at higher Reynolds number.

On the basis of these previous observations and the present study, it is suggested that a transformation exists between the near-wake structure induced by low amplitudes of the cylinder oscillation and that occurring at large amplitude. The nature of this transformation, in conjunction with force measurements, is currently under investigation.

ACKNOWLEDGEMENTS

REFERENCES

BEARMAN, P. W. 1984 Vortex shedding from oscillating bluff bodies. *Annual Review of Fluid Mechanics* **16,** 195–222.

BLACKBURN, H. M. & HENDERSON, R. D. 1995 Near-wake vorticity dynamics in bluff-body flows. *Proceedings of 12th Australiasian Fluid Mechanics Conference*, Sydney, December.

BROWN, G. L. & ROSHKO, A. 1974 On density effects and large structure in turbulent mixing layers. *Journal of Fluid Mechanics* **64,** 775–816.

COUDER, Y. & BASDEVANT, C. 1986 Experimental and numerical study of vortex couples in two-dimensional flows. *Journal of Fluid Mechanics* **173,** 225–251.

DETEMPLE-LAAKE, E. & ECKELMANN, H. 1989 Phenomenology of Kármán vortex streets in oscillating flow. *Experiments in Fluids* **7,** 217–227.

GRIFFIN, O. M. & HALL, M. S. 1991 Review—vortex shedding locked-on and flow control in bluff-body wakes. *ASME Journal of Fluids Engineering* **113,** 526–537.

GRIFFIN, O. M. & HALL, M. S. 1995 Vortex shedding lock-on in a circular cylinder wake. In *Flow-Induced Vibration* (ed. P. W. Bearman), pp. 3–14, *Proceedings of 6th International Conference on Flow-Induced Vibrations*, London, U.K. Rotterdam/Brookfield: A. A. Balkema Press.

GRIFFIN, O. M. & RAMBERG, S. E. 1974 The vortex streets of vibrating cylinders. *Journal of Fluid Mechanics* **66,** 553–576.

GU, W., CHYU, C. & ROCKWELL, D. 1994 Timing of vortex formation from an oscillating cylinder. *Physics of Fluids* **6,** 3677–3682.

HALL, M. S. & GRIFFIN, O. M. 1993 Vortex shedding and lock-on in a perturbed flow. *ASME Journal of Fluids Engineering* **115,** 283–291.

LIN, J.-C. & ROCKWELL, D. 1997 Quantitative interpretation of vortices from a cylinder oscillating in quiescent fluid. *Experiments in Fluids* **23,** 99–104.

LU, X. -Y. & DALTON, C. 1996 Calculation of the timing of vortex formation from an oscillating cylinder. *Journal of Fluids and Structures* **10,** 527–541.

ÖNGOEREN, A. & ROCKWELL, D. 1988 Flow structure from an oscillating cylinder. Part I, Mechanisms of phase shift and recovery of the near-wake. *Journal of Fluid Mechanics* **191,** 192–223.

ROCKWELL, D. 1990 Active control of globally-unstable separated flows. *International Symposium on Unsteady Flow Dynamics* (eds J. A. Miller & D. P. Telionis), Vol. FED-92, pp. 379–394. New York: ASME.

ROCKWELL, D. 1993 Quantitative visualization of bluff-body wakes by a particle image velocimetry. In *Bluff-Body Wakes, Dynamics and Instabilities* (eds H. Eckelmann, J. M. R. Graham, P. Huerre & P. A. Monkewitz), pp. 263–270. Berlin: Springer.

ROCKWELL, D., MAGNESS, C., TOWFIGHI, J., AKIN, O., & CORCORAN, T. 1993 High image-density particle image velocimetry using laser scanning techniques. *Experiments in Fluids* **14,** 181–192.

SARPKAYA, T. 1979 Vortex induced oscillations: A selective review. *Journal of Applied Mechanics* **46,** 241–258.

STAUBLI, T. & ROCKWELL, D. 1989 Pressure fluctuations on an oscillating trailing edge. *Journal of Fluid Mechanics* **203,** 307–346.

WILLIAMSON, C. H. K. & ROSHKO, A. 1988 Vortex formation in the wake of an oscillating cylinder. *Journal of Fluids and Structures* **2,** 355–381.

ZDRAVKOVICH, M. M. 1982 Modification of vortex shedding in the synchronization range. *ASME Journal of Fluids Engineering* **104,** 513–517.
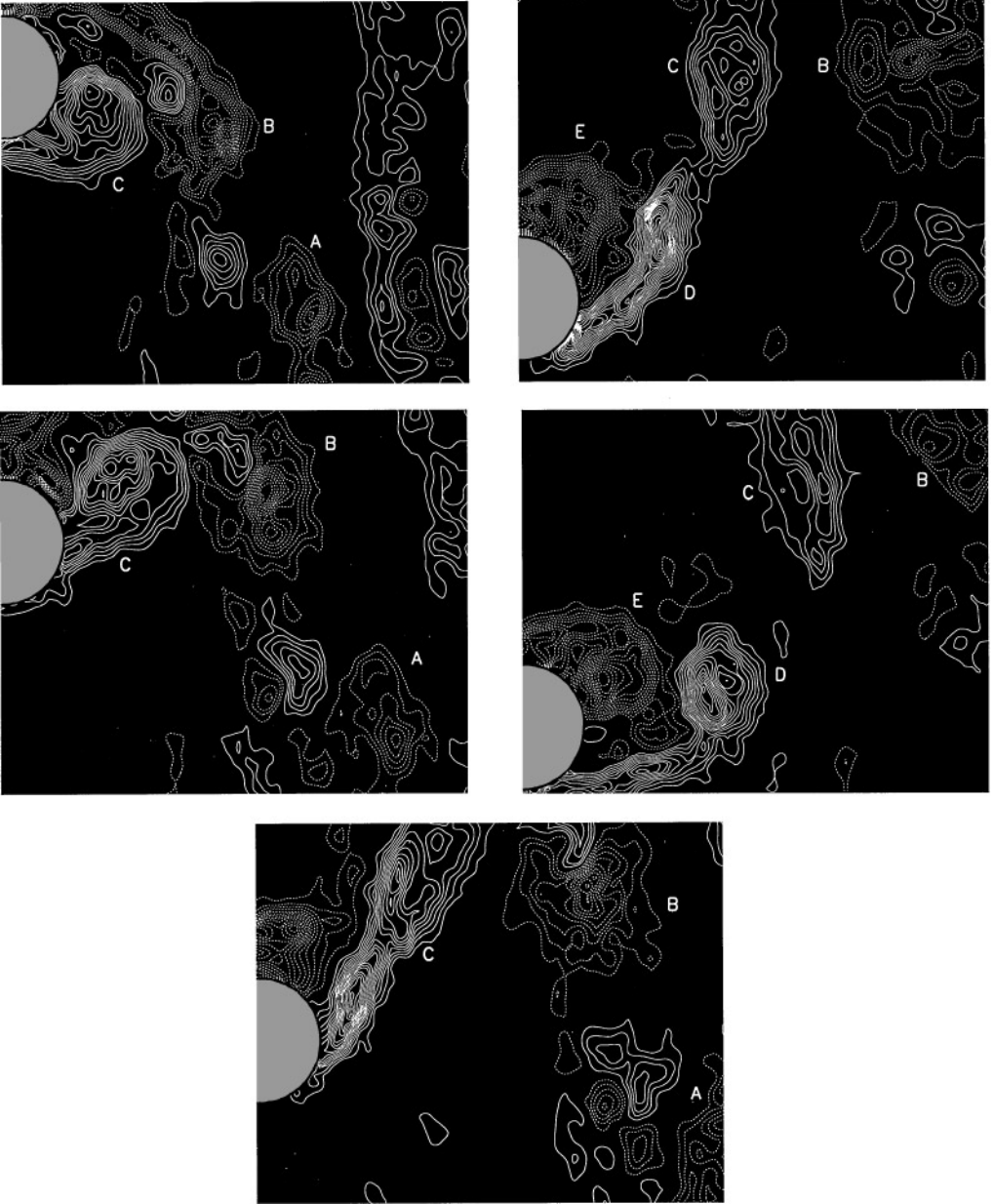
Figure 1. Vorticity contours in the near-wake of an oscillating cylinder. The cylinder moves from its maximum-positive to -negative position in the time sequence of images. Dimensionless amplitude is $A/D = 1 \cdot 0$ and frequency ratio is $f_e/f_0 = 1 \cdot 0$. Positive (solid line) and negative (dashed line) vorticity contours have minimum and incremental values, respectively, of $\omega_{min} = \pm\, 3\,\mathrm{s}^{-1}$ and $\varDelta\omega = 3\,\mathrm{s}^{-1}$.